

Inelastic neutron scattering studies of polyanilines and partially deuterated analogues

F. Fillaux ^{a,*}, N. Leygue ^a, R. Baddour-Hadjean ^a, S. Parker ^b, P. Colombari ^a,
A. Gruger ^a, A. Régis ^a, L.T. Yu ^c

^a *Laboratoire de Spectrochimie Infrarouge et Raman, Centre National de la Recherche Scientifique, 2 rue H. Dunant, 94320 Thiais, France*

^b *ISIS, Rutherford Appleton Laboratory, Chilton, Didcot, Oxon, OX11 0QX, UK*

^c *Laboratoire d'Electrochimie et Synthèse Organique, Centre National de la Recherche Scientifique, 2 rue H. Dunant, 94320 Thiais, France*

Received 14 October 1996

Abstract

Inelastic neutron scattering spectra have been measured from 16 to 4000 cm^{-1} for various polyaniline samples at 30 K: the emeraldine-base and the emeraldine-salt, the ring-deuterated analogues and their hydrated forms. The spectra of the totally hydrogenated samples are dominated by bands due to protons bound to the aromatic rings. The spectrum of the ring-deuterated base reveals that most of the remaining protons are not bound to nitrogen atoms. There is a continuum of intensity due to the recoil of free particles with mass 1 amu. In the emeraldine-salt additional protons (H^+) are trapped in very shallow potential-wells with dissociation threshold $\sim 300 \text{ cm}^{-1}$. At energy transfer greater than this threshold, these protons are free to recoil. The spectra of the hydrated samples reveal that free entities are not trapped by water molecules. These new dynamics are tentatively related to the electronic structure and conductivity of these polymers. These are supposed to be determined by the position of the electronic state of “ H^{0+} ” entities relatively to the half-filled π -band of the metal-like form of the pernigraniline-base. In the emeraldine-base electrons transferred from “ H^{0+} ” entities to the conduction band give an insulator with a totally-filled band and a gas of H^+ entities. In the emeraldine-salt the electronic state of “ H^{0+} ” entities is lowered. The structure is that of a metal-like half-filled band with a gas of “ H^{0+} ” entities and weakly bound protons.

Keywords: polyaniline; emeraldine; inelastic neutron scattering; free protons

1. Introduction

Polyanilines obtained from mild oxidation of aniline in acidic media are unusual members of the class of conducting polymers. For many other members of this class (e.g., polyacetylene, polydiacetylene and polythiophene) electronic properties are well

understood by considering their conjugated carbon backbones [1,2]. This is not the case for polyanilines where protonation of the nitrogen atoms gives access to several derivatives with changes of electronic conductivity (σ) over ten orders of magnitude, ranging from insulators or semiconductors (e.g., the emeraldine-base with $\sigma < 10^{-6} \text{ S cm}^{-1}$) to metal-like (e.g., the emeraldine-salt with $\sigma > 10^{-1} \text{ S cm}^{-1}$), depending upon the oxidation level, the pro-

* Corresponding author.

tonation degree and the hydration state [3–11]. The metal-like form is also a proton conductor ($\sigma_{\text{ionic}} \sim 10^{-2} \text{ S cm}^{-1}$) [7]. Various models have been proposed to account for this particular behaviour [12].

The term ‘‘polyaniline’’ is descriptive of a class of polymers derived from the virtually non-conducting base forms which are represented as mixtures of benzoid and quinoid entities (*p*-phenylenamineimine) according to the general chemical formula (I) in Scheme 1. This view is supported by experimental techniques such as infrared and Raman [13,14] and CPMAS NMR [15,16]. The averaged oxidation state, given by the parameter x_0 , depends on the synthesis process. This can be varied from $x_0 = 0$ (leucoemeraldine) to $x_0 = 1$ (permigraniline). The polymerisation degree, n , is difficult to measure since polyanilines are almost insoluble in organic solvents. However, spectroscopic studies revealed no significant contribution of end-groups [17].

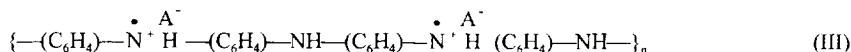
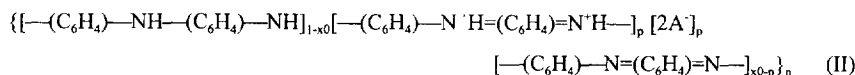
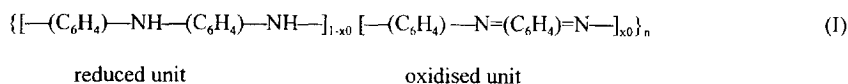
The emeraldine-base consists of equal numbers of reduced and oxidised repeat units ($x_0 = 0.5$). It has been suggested that this polymer tends to be composed mainly of alternating amine and imine units [17,18]. Clustering of only those units which are present in larger number occurs in samples having oxidation states $x_0 \neq 0.5$.

Polyanilines are unique among conducting polymers in that the base-forms (I) having $x_0 > 0$ are in a partially oxidised-state, even though there is no excess charge on the backbone. Thus these forms can be doped by nonoxidising protonic-acids. Protonation is supposed to increase hydrogen-bearing nitrogen atoms at the expense of the imine form. Imine

nitrogen atoms ($\text{N}=\text{}$) are protonated and positive charge is transferred to the backbone. Mobile charge carriers are generated after internal reorganisation of the electron density [18]. The emeraldine-salt containing a fraction p of protonated imine-quinone groups is represented with bipolaron entities [formula (II) in Scheme 1]. With strong acids, like HClO_4 , HCl or H_2SO_4 , all the imine-quinone groups are protonated ($p = x_0$). For these emeraldine-salts the conductivity at room temperature is increased by ~ 10 orders of magnitude and a metal-like Pauli paramagnetic-susceptibility appears [19]. XPS, EPR and NMR measurements [19–22] suggest that most of the electric charges are on the N and not on the C atoms. It has been proposed that disproportionation of the protonated polymer (II) gives mainly the semiquinone-radical cations or polarons. In the particular case where $x_0 = 0.5$, this can be written as formula (III) in Scheme 1. In this formal structure, the unpaired electron spins are believed to reside mainly on the nitrogen atoms located near the counter ions A^- . Charge hopping among fixed polaron and bipolaron sites could be the primary charge-transport mechanism in the lightly protonated emeraldine-bases [19]. At high protonation (doping) levels, polarons are arrayed to form a lattice with metal-like transport within the partially-filled polaron energy-band.

Amine nitrogen can also be protonated, but this process does not contribute charge to the system [18].

Though the key role of protonation in conducting properties of polyanilines was largely evidenced, studies of the proton dynamics are rather limited



Scheme 1. Chemical formula for various polyanilines.

[23–28]. Infrared spectra of the $\sim 50\%$ protonated base (metal-like) revealed an intense and broad band at $\sim 1100\text{ cm}^{-1}$ with sharp transmission windows whose frequencies correspond to narrow Raman bands [26,27]. This band was tentatively assigned to the proton stretching-mode of a rather strong N...H...N hydrogen bond with N...N $\sim 2.5\text{ \AA}$. This was thought to support the polaronic model, and systematic studies suggest that this band and the electronic conductivity appear simultaneously. However, this band is only slightly changed upon deuteration and alternative interpretations cannot be ruled out. Besides, hydrated polyaniline (up to ~ 20 weight%) showed no significant change in the infrared despite a slight increase of conductivity. More recently, it has been shown that spectra in the infrared are dominated by reflection rather than absorption and data were re-analysed consequently [28]. However, since the various signals cannot be distinguished easily, infrared spectroscopy provides ambiguous information, that concerns primarily the surface of the polyaniline samples. Raman spectroscopy, on the other hand, is hampered by resonance effects due to the very broad electronic absorption from UV to near infrared.

Inelastic neutron-scattering (INS) spectroscopy is the only technique which may provide clear information on proton dynamics in polyanilines. Because the scattering cross-section of hydrogen atoms is about ten times greater than that for C and N atoms, the spectra are dominated by signals due to proton motions, and totally free of side effects encountered with optical techniques (namely, reflection or resonance). This proton selectivity can be further exploited because deuterium atoms have a very much smaller cross-section than protons. Specific deuteration of the conjugated rings provides a detailed view of the dynamics for protons involved in the conduction mechanisms. Therefore, INS is anticipated to give simpler spectra which can be analysed with more confidence. So far, proton dynamics in polyanilines have been studied only partially with INS [29,30]. Previous spectra obtained with fully hydrogenated samples were dominated by bands involving the CH groups and it was difficult to identify bands specific to mobile protons. INS spectra of partially-deuterated materials are of great interest in this context.

We have thus undertaken INS studies of polyanilines and their ring-deuterated analogues with various protonation and hydration degrees. In this present paper, we report spectra of the emeraldine-base ($x_0 = 0.5$, $p = 0$), emeraldine-salt ($x_0 = 0.5$, $p = 0.5$) and the hydrated analogues.

2. Experimental

The emeraldine-salt (SH) and its ring-deuterated analogue (SD) were chemically prepared in solutions containing sulphuric acid [31]. Aniline was purified by trap to trap distillation under dried argon-atmosphere. 12 cm^3 of aniline were added to 150 ml of 1.5 N HCl. A solution containing 30 g of ammonium persulfate, $(\text{NH}_4)_2\text{S}_2\text{O}_8$, in 150 ml of 1.5 N HCl was added slowly at $\sim 0^\circ\text{C}$. The polymer was then filtrated and washed with water and methanol. The emeraldine-base (BH) and the ring-deuterated analogue (BD) were obtained after neutralisation of the corresponding salts with ammonia in aqueous solution. The salts were obtained from solutions in HCl 0.5 N. Another sample (S'H) was cast from a solution in H_2SO_4 at 95% with CH_3OH . The hydrated samples were obtained after desiccation under static vacuum. The dried samples were pumped under vacuum until constant weight. The loss of weight was $\sim 60\%$. Elemental analyses (Table 1) are in accord with the chemical formula of polyanilines, within $\sim 7\%$. For the emeraldine-salt the amounts of Cl atoms confirm the anticipated protonation degree: $p = 0.5 \pm 0.05$. The amount of water is much greater for the salt than for the base.

INS spectra were obtained with the TFXA-spectrometer at the ISIS pulsed neutron-source (Ruther-

Table 1
Elemental analysis in weight % of the fully hydrogenated polyanilines dried under vacuum. See Section 2

Sample	C	H	N	O	Cl	H_2O	Stoichiometry (approximated)
Salt (SH)	53.6	5.2	10.6	13.5	12.0	14.1	$\sim (\text{C}_6\text{H}_4\text{NH}\cdot\text{H}_2\text{O})_n$
Salt (S'H)	53.8	5.1	10.9	13.8	11.6	13.7	$\sim (\text{C}_6\text{H}_4\text{NH};\text{H}_2\text{O})_n$
Base (BH)	75.1	5.0	14.5	4.2	0.2	2.6	$\sim (\text{C}_6\text{H}_4\text{NH};0.25\text{H}_2\text{O})_n$

ford Appleton Laboratory, Chilton, UK). The resolution was $\Delta\omega/\omega \sim 2\%$. About 5 g of sample were wrapped in aluminium foil and then loaded in a closed-cycle refrigerator at ~ 30 K. Spectra were converted from time-of-flight to energy-transfer according to standard procedures. Intensities were renormalised according to the amount of sample in the beam.

3. INS spectra and proton dynamics

3.1. Emeraldine-salts

The INS spectra of the fully-hydrogenated emeraldine-salts prepared by two different synthesis routes (Fig. 1A and Fig. 2) are quite similar. They are dominated by well defined bands between 400 and 2000 cm^{-1} due to CH bending (out-of-plane at 820 and 975 cm^{-1} , in-plane at 1170 and 1275–1350 cm^{-1} , see Table 2) and aromatic-ring modes (420, 525, 610 and 720 cm^{-1}). Weak bands at about 1500 cm^{-1} may correspond to CN or CC-stretching modes mixed with CH vibrations. The CH-stretching modes are clearly observed at ~ 3150 cm^{-1} .

Weak bands at 280 and 345 cm^{-1} are assigned to vibrational modes of the polymer chains. Below 200 cm^{-1} rather broad density-of-states are observed for the lattice modes. INS intensities for the modes of the aromatic rings and polymer backbone are due to dynamical coupling to proton vibrations and/or proton-riding effects. Below ~ 400 cm^{-1} the INS spectra in Fig. 1A and Fig. 2 are almost identical. Only tiny differences are observed for the very weak

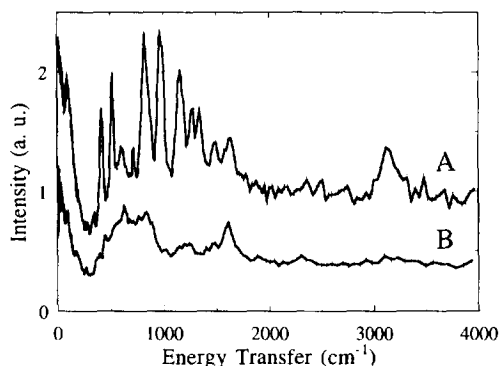


Fig. 1. INS spectra of the emeraldine-salt at 30 K. A: totally hydrogenated (SH). B: ring deuterated (SD).

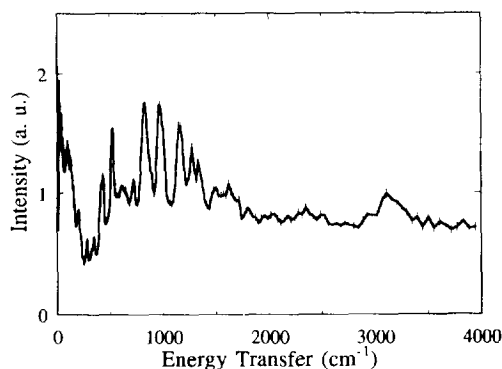


Fig. 2. INS spectrum of the emeraldine-salt (S'H), cast from sulfuric acid, at 30 K.

bands at 280 and 345 cm^{-1} . Structures and dynamics, as revealed by INS, are almost independent of the synthesis process.

For the ring-deuterated analogue (Fig. 1B), all the bands due to CH-modes coupled to the ring vibrations are shifted downwards below 1000 cm^{-1} . As

Table 2

Band frequencies (cm^{-1}) and tentative assignments for the fully hydrogenated emeraldine-base and salt (h_5) and their partially deuterated analogues (hd_4) at 30 K

Salt- h_5	Salt- hd_4	Base- h_5	Base- hd_4	Assignments
90m	90w	95m	95w	lattice
380vw	385vw	380vw	380vw	chain + ring + CH bending
420m	460vw	425m	440vw	chain + ring + CH bending
525m	—	530m	—	ring + CH bending
610w	—	592vw	—	ring
—	—	637vw	—	ring
720w	—	720w	—	ring
—	630w	—	630w	$\gamma\text{CD} + \text{H}_2\text{O}$
820s	—	830s	—	γCH
980s	—	960s	—	γCH
—	845w	—	830w	δCD
—	—	—	1035w	—
—	—	1134m	—	$\delta\text{CH} + \text{ring} + \nu\text{CN}$
1175s	—	1180s	—	$\delta\text{CH} + \text{ring} + \nu\text{CN}$
1280m	—	1300m	—	$\delta\text{CH} + \text{ring} + \nu\text{CN}$
1350m	—	1400w	—	$\delta\text{CH} + \text{ring} + \nu\text{CN}$
—	1230vw	—	1230vw	H_2O
1500w	1500vw	1500w	1500vw	$\nu\text{CN} + \delta\text{CH} + \text{ring}$
1635m	1630m	1630w	1635w	H_2O
—	2330vw	—	2335vw	νCD
3150m	—	3125	—	νCH

s: strong; m: medium; w: weak; v: very.

anticipated, intensities of CD modes are dramatically weaker than those of CH modes. The CD-bending modes give weak bands at 630, 845 and 1035 cm^{-1} , on the top of a broad band extending itself from 400 to 1000 cm^{-1} . From the frequency point of view, this band and weaker bands at 1225 and 1630 cm^{-1} might correspond to the proton stretching and bending modes of rather strong hydrogen bonds [32,33]. However, intensities do not confirm this assignment scheme. The broad band from 400 to 1000 cm^{-1} is much more intense than the band at 1630 cm^{-1} which is itself more intense than the band at 1225 cm^{-1} . In contrast to this, similar intensities have been observed for the three proton modes in hydrogen-bond complexes [34,35]. Finally, these bands are more likely due to water molecules in accord with the elemental analysis (Table 1), and, eventually, to very small amounts of protons engaged in strong hydrogen bonds (e.g., N...H...N). It is likely that these features already exist in the fully hydrogenated sample, underneath the CH-bands.

For all samples, there is a continuum of intensity underneath the bands discussed above. By analogy to previous works [36–39], this continuum is attributed to the recoil of free particles with mass ~ 1 amu. This is the most straightforward evidence for mobile proton-like entities in polyaniline. In the observed spectral-range, there is no visible intensity cut-off at low frequency. Therefore, these particles are not bound to any local potential-well with dissociation threshold greater than ~ 20 cm^{-1} . They behave as a gas of free particles. However, INS does not provide any information on the effective electric-charge of the recoiling entities. It is not possible to distinguish between H^+ , H^0 and H^- , or any intermediate entity.

The intensity of the continuum is significantly depressed in the ring-deuterated sample, compared to the fully-hydrogenated one. A naive interpretation would conclude that there are less free entities in the deuterated sample. However, ring protons are not anticipated to contribute to recoil. Moreover, the INS spectra confirm that CD groups do not exchange spontaneously with protons. Therefore, ring-deuteration does not affect the amount of mobile entities. In line with previous works [38,39], this decrease of intensity is a consequence of the Doppler broadening of the recoil spectrum along the momentum-transfer coordinate (see Section 4).

Table 3

Comparison of INS integrated intensities in arbitrary units for the emeraldine-salt. I_0 is the spectral intensity integrated from 16 to 4000 cm^{-1} , normalized for 10 g of sample in the beam. I_1 is the intensity after subtraction of the continuum. I_c is the integrated intensity for the continuums. p_0 and p_1 are the estimated numbers of protons per chemical formula units. Stoichiometries are those obtained from elemental analysis (see Table 1)

	Salt	
	$(\text{C}_6\text{H}_4\text{NH}\cdot\text{H}_2\text{O})_n$	$(\text{C}_6\text{D}_4\text{NH}\cdot\text{H}_2\text{O})_n$
I_0	4730 ± 17	1940 ± 8
p_0	6.8 (~ 7)	2.8 (~ 3)
I_1	2060 ± 34	750 ± 16
p_1	6.3 (~ 6)	2.3 (~ 2)
I_c	2670 ± 34	1190 ± 16

For the ring-deuterated emeraldine-salt, bands that could be attributed to protons bound to N atoms are almost invisible. Compared to the fully-hydrogenated analogue, 1/5 protons remains in the partially-deuterated sample. Therefore, if protons were bound to N atoms, each mode intensity should be comparable to one of those bands corresponding to the CH-bending modes in the fully-hydrogenated derivative. The band at 1630 cm^{-1} is too weak to correspond to a single degree of freedom. Compared to the CH-mode intensity, we estimate that this band would correspond to only $\sim 25\%$ of protons bound to nitrogen atoms, if the contribution of water molecules is neglected. Consequently, the actual value is probably very much less. Most of the protons are free and contribute to the continuum intensity.

This is confirmed with INS intensities. The difference between intensities integrated over the whole spectral-range (I_0 in Table 3) for the fully-hydrogenated salt and its deuterated analogue corresponds to the contribution of the four protons bound to the aromatic rings. This gives the averaged intensity per CH-mode of $\sim 700 \pm 10$ a.u. The amounts of protons in the samples calculated with this value (p_0 in Table 3) compare very favourably to the elemental analyses (Table 1). The same analysis was performed with integrated intensities after subtraction of the continuum defined as an horizontal line at the minimum intensity for each spectrum (I_1 in Table 3). The estimated numbers (p_1 in Table 3) confirm that only a minor fraction of protons is bound to the

nitrogen atoms. Finally, it is confirmed that the continuum is approximately twice more intense for the fully-hydrogenated sample than for the ring-deuterated one (see below).

3.2. Emeraldine-base

The INS spectra of the emeraldine-bases (Fig. 3) are very similar to those of the corresponding salts. For the fully hydrogenated sample (Fig. 3A), the main bands due to CH bending and ring modes are slightly broader. Some of them reveal partially resolved structures which could be related to the mixture of benzoic and quinoidal rings [see formula (I) in Scheme 1]. However, the lack of significant frequency-shift for the modes of the aromatic rings at 420, 520, 610 and 720 cm^{-1} precludes a clear identification of these two forms. Furthermore, it is not straightforward to rationalise the evolution of the proton bending-modes in terms of two distinct chemical species. The CH out-of-plane bending at 955 cm^{-1} is shifted downwards by $\sim 20 \text{ cm}^{-1}$, compared to the salt, whilst the other out-of-plane bending at 830 cm^{-1} is virtually unchanged. The CH in-plane bending, observed previously at 1160 cm^{-1} for the salt (Fig. 1A), splits into two bands at 1130 and 1185 cm^{-1} in the emeraldine-base. On the other hand, the doublet at 1275–1350 cm^{-1} for the salt merges into a single band at 1315 cm^{-1} for the base (Fig. 3A). Surprisingly, the bands at about 1500 cm^{-1} containing CC and/or CN stretching vibrations are not affected by protonation. The CH stretching is shifted downwards by $\sim 40 \text{ cm}^{-1}$ in

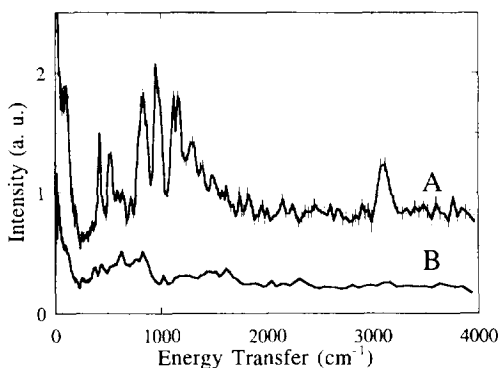


Fig. 3. INS spectra of the emeraldine-base at 30 K. A: totally hydrogenated (BH). B: ring deuterated (BD).

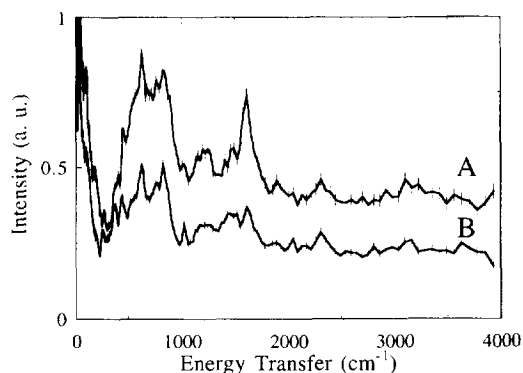


Fig. 4. Comparison of the INS spectra of the partially deuterated emeraldine-salt (SD, curve A) and base (BD, curve B) at 30 K.

the emeraldine-base. Chain modes and lattice density-of-states below 350 cm^{-1} are very similar for all samples. There is no obvious relationship between these observations and the molecular structure (I).

The broad band between 400 and 1000 cm^{-1} , including the weak ring-deuterated modes, and bands at 1225 and 1630 cm^{-1} are similar to those observed for the salt, but much weaker. This is in line with the much smaller amount of water in the base (see Table 1). There is virtually no evidence for protons bound to nitrogen atoms. The continuum of intensity due to recoil of free particles with mass $\sim 1 \text{ amu}$ is still clearly observed.

A detailed comparison of the spectra of the partially-deuterated emeraldives (Fig. 4) reveals that the continuum of intensity is a minimum at $\sim 300 \text{ cm}^{-1}$ for the salt, whereas it is approximately a constant

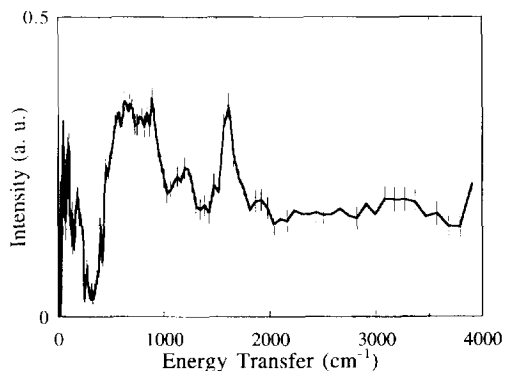


Fig. 5. Difference spectrum obtained after subtraction of the spectrum of the emeraldine-base (Fig. 3B) from that of the emeraldine-salt (Fig. 1B).

for the base. This view is confirmed with the difference spectrum of the two samples (Fig. 5). At $\sim 300 \text{ cm}^{-1}$, intensities are virtually equal for both samples. Below this frequency, the density-of-states are superimposed to the continuum of the base. Above $\sim 300 \text{ cm}^{-1}$, the continuum intensity remains approximately a constant for the base, whilst it increases for the salt. These observations suggest that the recoiling particles are totally free in the base, whilst additional protons in the salt are bound in shallow potential-wells with dissociation thresholds of $\sim 300 \text{ cm}^{-1}$ (see below).

3.3. Hydrated samples

The INS spectrum of the hydrated emeraldine-salt (Fig. 6) is dominated by bands specific to a rather well crystallised form of water, similar to Ice Ih [40,41]. In the translational region (below 400 cm^{-1}), the acoustic modes give a very sharp peak at $\sim 56 \text{ cm}^{-1}$ with a very weak shoulder at $\sim 100 \text{ cm}^{-1}$. The weaker peaks at 141, 228 and $285\text{--}307 \text{ cm}^{-1}$ have been attributed to O...O stretching modes [40]. All these bands have counterparts in the infrared and Raman spectra of Ice Ih. At higher frequency, the density-of-states of the optic molecular modes of Ice Ih are observed between ~ 500 and 1100 cm^{-1} with the very sharp low energy cut-off at $\sim 550 \text{ cm}^{-1}$ and maxima at 570, 640, 830 and 960 cm^{-1} . They correspond to librations of water molecules. The broad band at $\sim 1600 \text{ cm}^{-1}$ is attributed to the internal bending-mode of water molecules. Ill-de-

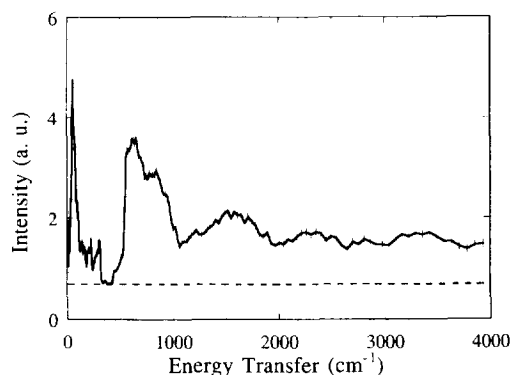


Fig. 7. INS spectrum of the hydrated emeraldine-base (BH) at 30 K. The dashed line defines the continuum of intensity tentatively attributed to proton recoil.

fined broad bands above 2000 cm^{-1} are due to overtones and combinations. The stretching modes are barely visible at $\sim 3300 \text{ cm}^{-1}$.

The spectrum of the hydrated emeraldine-base (Fig. 7) is also dominated by bands due to crystallised ice-like water. The main difference between the two spectra is a significant decrease of intensity above $\sim 600 \text{ cm}^{-1}$ for the non-protonated sample compared to the protonated one (compare Figs. 6 and 7).

Finally, these spectra reveal continuums of intensity very similar to those observed for the dried samples. Therefore, the dynamics of free particle is not significantly changed by water molecules.

4. Proton recoil

In order to analyse the dynamics of free particles in polyanilines, it is necessary to refer to previous INS works with the TFXA-spectrometer on manganese dioxide ($\gamma\text{-MnO}_2$) [36], which is also a proton conductor, and coals [37] that have revealed a similar recoil of particles with mass $\sim 1 \text{ amu}$. These entities are not chemically bound to any particular atom. Instead, they behave as gas of free particles. Because the final state is free, neutrons are scattered at any energy-transfer values and give a continuum of intensity. In contrast to this, discrete energy-transfer values occur for bound oscillators.

A major limitation of the TFXA spectrometer is that momentum (Q) and energy-transfer ($\hbar\omega$) are

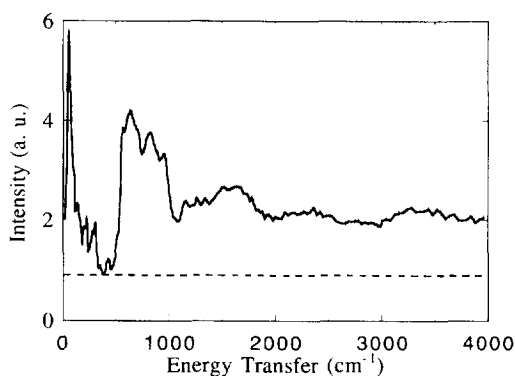


Fig. 6. INS spectrum of the hydrated emeraldine-salt (SH) at 30 K. The dashed line defines the continuum of intensity tentatively attributed to proton recoil.

correlated according to: $\hbar\omega \sim 16Q^2$ (with the energy and momentum transfer in cm^{-1} and \AA^{-1} units, respectively). Q is the vector difference between the incident and scattered wave-vectors $|k_i| = 2\pi/\lambda_i$ and $|k_j| = 2\pi/\lambda_j$, where λ_i and λ_j are the incident and scattered wave-lengths, respectively. This trajectory in the (Q, ω) space, corresponds to the maximum in the scattering-function for particles with mass ~ 1 amu, either oscillating (bound) or recoiling (free) and is often referred to as the “proton recoil line”. However, measurements over a large range of momentum-transfer provide a detailed view of the dynamics of free entities [38,39]. The variation of the INS spectral intensity with Q (i.e., the angle at which the scattered neutrons are measured) yields the full scattering-function $S(Q, \omega)$ which contains spatial information on the wave-function.

For free particles, the scattering function can be calculated within the impulse approximation, [42,43]:

$$S(Q, \omega) = \int n(\mathbf{p}) \delta\left(\hbar\omega + \frac{\hbar^2}{2m}p^2 - \frac{\hbar^2}{2m}(\mathbf{p} + \mathbf{Q})^2\right) d\mathbf{p} \quad (1)$$

The δ function expresses the conservation of the kinetic energy which applies to the collision between the nucleus with mass m and the neutron [42]. The kinetic-momentum distribution in the ground state is $n(\mathbf{p})$. In this section, we shall consider two models: the gas of free particles and particles in a shallow potential well. A more detailed discussion is presented in Ref. [39].

4.1. Gas of free particles

For a gas of free particles with the Maxwell–Boltzmann distribution of kinetic-momentum, the scattering-law is [42,43]:

$$S(Q, \omega) = \left(\frac{1}{4\pi E_R kT}\right)^{1/2} \exp\left[-\frac{1}{4E_R kT}(\hbar\omega - E_R)^2\right] \quad (2)$$

where:

$$E_R = \hbar\omega_R = \frac{\hbar^2 Q^2}{2m} \quad (3)$$

E_R is the recoil energy. The INS spectrum of such particles is a ridge of intensity which is a maximum along the recoil line defined by Eq. (3). Since the TFXA-spectrometer measures the narrow slice of (Q, ω) space along the recoil line for $m = 1$ amu, free protons manifest themselves as a continuum with maximum of intensity proportional to $(E_R kT)^{-1/2}$. Alternatively, for effective masses greater than 1 amu, the TFXA-spectrometer gives parabolic spectral profiles for recoiling entities [44].

$S(Q, \omega)$ maps of intensity previously obtained for coals [38] and $\gamma\text{-MnO}_2$ [39] have revealed that the width of the recoil line is more than one order of magnitude greater than that anticipated for an isolated gas of free protons at the temperature of the sample. Different models have been considered: ideal gas obeying Maxwell–Boltzmann or Fermi statistics, multiple scattering, phonon wings, protons trapped in shallow potentials and quantum correlations between free and bound protons. None of them is satisfactory. Finally, Doppler broadening by the zero-point motions of the lattice provides a satisfactory theoretical framework to represent recoil spectra. Free particles are represented as planar-waves with kinetic momentum distribution $n_H(\mathbf{p}_H)$ corresponding to that of an ideal gas at thermal equilibrium. At very low temperature particles are virtually at rest with respect to the lattice referential which is still oscillating with respect to a “fixed” laboratory-frame. This corresponds essentially to the zero-point energy of the lattice modes. These collective oscillations are represented as phonons, i.e., planar-waves, with distribution of kinetic momentum:

$$n_L(\mathbf{p}_L) = \left(\frac{2\langle U_L^2 \rangle}{\pi}\right)^{1/2} \exp(-2p_L^2 \langle U_L^2 \rangle) \quad (4)$$

where $\langle U_L^2 \rangle$ is the averaged mean-square amplitude of the lattice modes. All together, $n_L(\mathbf{p}_L)$ and $n_H(\mathbf{p}_H)$ form the total density-of-states which is probed by neutrons. The scattering-function is merely the convolution of the recoil spectrum for a gas of protons with the kinetic-momentum distribution of the lattice modes. For $mkT \ll (\langle U_L^2 \rangle)^{-1}$:

$$S(Q, \omega) \propto \exp\left[-2\left(|Q| - \frac{\sqrt{2ME_R}}{\hbar}\right)\langle U_L^2 \rangle\right] \times \delta(\hbar\omega - E_R) \quad (5)$$

The intensity at maximum is largely independent of the energy-transfer value, in accord with the INS spectra. This broadening mechanism can be compared to the Doppler effect. The wave-vector for the incident neutrons is defined with respect to a “fixed” laboratory referential. For a given value \mathbf{p}_L , the incoming wave-vector experienced by free protons ($\mathbf{k}_i - \mathbf{p}_L$) is either blue or red shifted, depending on the mutual orientation of the two vectors. The momentum effectively transferred to free particles ($\mathbf{Q}_H = \mathbf{k}_i - \mathbf{p}_L - \mathbf{k}_f$) is different from that transferred to the whole sample: $\mathbf{Q} = \mathbf{k}_i - \mathbf{k}_f$.

Within the harmonic approximation, $\langle U_L^2 \rangle \propto \langle \sum_i \mu_i \nu_i \rangle^{-1}$, where μ_i and ν_i are the effective masses and frequencies for lattice modes. Because C and N atoms are much heavier than protons, the averaged mean-square amplitude for lattice modes is largely dominated by modes due to bound protons and with mean square amplitude $\langle u_B^2 \rangle \sim 1 \times 10^{-2} \text{ \AA}^2$. Therefore, $\langle U_L^2 \rangle \sim \langle u_B^2 \rangle \sim 1 \times 10^{-2} \text{ \AA}^2$. For the partially deuterated samples, the averaged mean-square amplitudes for lattice modes are dominated by deuterium atoms and $\langle U_L^2 \rangle$ is roughly divided by a factor two. Therefore, according to Eq. (4), the width of the recoil line is about twice larger for the partially deuterated sample compared to the totally hydrogenated derivative. Consequently, the intensity at maximum is divided by a factor ~ 2 upon deuteration. This mechanism accounts for the much lower continuum intensity for the ring-deuterated samples compared to the fully hydrogenated analogues (see Figs. 1 and 3, and Table 3).

4.2. Shallow potential with a single bound state

A detailed comparison of the spectra of the partially deuterated samples (Figs. 5 and 6) reveals different proton dynamics. Above 300 cm^{-1} the continuum intensity for the salt is approximately twice that for the base, as anticipated if most of the protons recoil at high energy transfer. However, spectral intensities around 300 cm^{-1} are very similar for the two samples (Fig. 5) and the difference spectrum confirms a dip of intensity in this region for protons added to the salt (Fig. 6). This suggests that these protons are trapped in a shallow potential with a single bound (ground) state located $\sim 300 \text{ cm}^{-1}$ below the dissociation threshold (schemati-

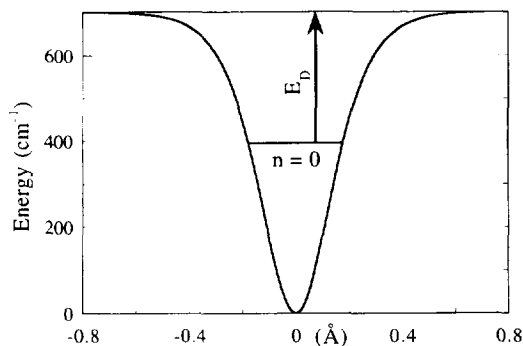


Fig. 8. Shallow potential function with a single bound-state, $n = 0$: $V(x) = 700(1 - 1/\cosh^2(5.5x))$; V and x are in cm^{-1} and \AA units, respectively. The bound state is at $\sim 300 \text{ cm}^{-1}$ and $E_D \sim 300 \text{ cm}^{-1}$ is the dissociation energy.

cally represented in Fig. 8). In this case, we can distinguish two dynamical regimes: localised protons for $\hbar\omega < E_D$ and recoil for $\hbar\omega > E_D$.

At large energy-transfer, the scattering-law for transitions from the ground state to the continuum can be calculated within the impulse approximation which applies provided the final state is free [42]. In the isotropic harmonic case:

$$S(Q, \omega) \approx \left(\frac{m}{4\pi E_R u^2} \right)^{1/2} \exp \left[- \frac{m}{4E_R u^2} (\hbar\omega - E_R)^2 \right];$$

$$\hbar\omega > E_R \quad (6)$$

This equation is similar to Eq. (2) with $u^2 = mkT$, where u^2 is the mean square-amplitude in the ground state. At low energy-transfer ($\hbar\omega < E_D$) a cut-off of intensity is anticipated. The dip of intensity observed at $\sim 300 \text{ cm}^{-1}$ (Fig. 6) may correspond to $\sim E_D$. Unfortunately, this is not sufficient for a full determination of the potential function in Fig. 8 which includes at least 2 parameters. However, the spectra provides some qualitative information. The continuum above 2000 cm^{-1} (Fig. 5) has almost constant intensity, whereas it should decrease at high energy transfer as $E^{-1/2}$, according to Eq. (6). This suggests that the width of the recoil line is dominated by Doppler broadening. This may occur if $u^2 \ll \langle U_L^2 \rangle$. Consequently the potential minimum must be rather flat and the wave-function in the ground state rather extended.

5. Discussion

The existence of free particles with effective mass of 1 amu in polyanilines is certainly one of the most significant output of the present work. It appears that the naive chemical formulae (I, II and III in Scheme 1) do not reflect the real localisation and dynamics of protons since most of the protons associated to the averaged oxidation state x_0 are not bound to N atoms. The spectra reveal that they are largely delocalised. It is then logical to speculate that the corresponding electrons are also delocalised. This is in line with the fact that phenyleneamine and phenyleneimine entities cannot be distinguished on the time-scale of INS measurements (10^{-12} – 10^{-15} s).

Therefore, a major conclusion of this work is that the emeraldine-base can be regarded as the pernigraniline-base

graniline-like structure interacting with a gas of free hydrogen atoms “ H^0 ”. The resulting electronic structure is determined by the relative positions of the electronic states for “ H^0 ” and, less likely “ H^- ”, entities with respect to those for the pernigraniline base (see Fig. 9). These electronic states might be regarded as extremely narrow band structures.

The fully conjugated form of the pernigraniline-base is a half-filled band system with metal-like band-structure (pernigraniline-M or P-M in Fig. 9a). However, it is anticipated to undergo dimerisation to a semiconducting Peierls ground-state (pernigraniline-SC or P-SC in Fig. 9b). Then, the half-filled π -band of P-M, estimated to have a width of 2.9 eV, is split by a calculated energy-gap of 1.4 eV caused by an effective bond-length alternation analogous to the single-bond double-bond alternation in dimerised trans polyacetylene [45].

The emeraldine-base (Fig. 9c) can be seen as the insulator analogue of the pernigraniline-M. The additional electrons in the now totally-filled band are provided by the hydrogen atoms. This occurs if the electronic state of the “ H^0 ” entities is at a greater energy than the top of the electronic band of P-M. The conducting band is totally filled for $x_0 \geq 0.5$. In the case where $x_0 \sim 0.5$, the recoiling particles are essentially H^+ entities and proton conduction is possible. Therefore, within this scheme the emeraldine base is an electronic insulator and could be a proton conductor. Moreover, the emeraldine-base gives two absorption bands due to electronic transitions at 3.8 and 2.0 eV, respectively [46,47]. The former corresponds to the π – π^* transition. The band at 2.0 eV was assigned to internal charge transfer associated with excitations from benzoid to quinoid moieties. In the diagram presented in Fig. 9c it is straightforward to assign this band to the transfer of electrons from the polymer conduction band to free protons (H^+) to form free hydrogen atoms “ H^0 ”.

To account for the metal-like conduction of the emeraldine-salt, the protonation of the emeraldine-base should lower the electronic state of “ H^0 ” below the top of the conduction band. Electrons are then transferred from the electronic-band to protons H^+ to give “ H^0 ” (Fig. 9d). The emeraldine-salt (with protonation degree $p = 0.5$) is thus a half-filled

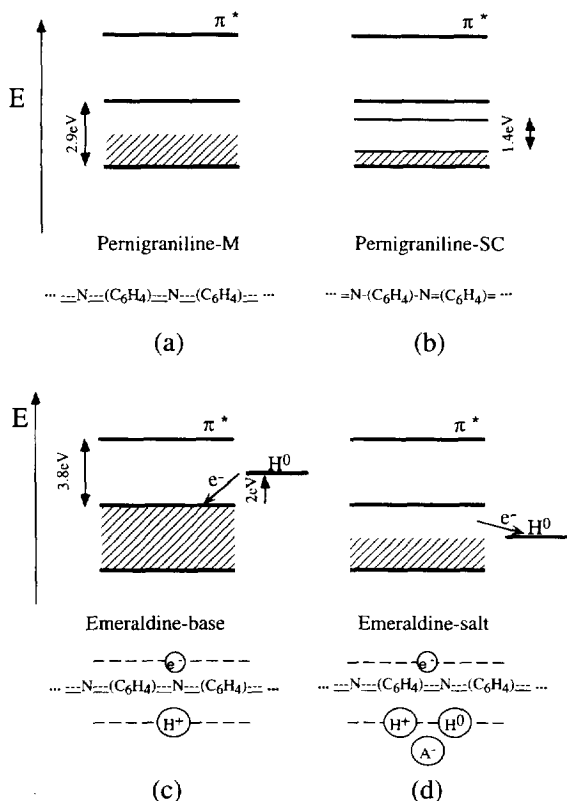


Fig. 9. Schematic energy-diagrams for the electronic states of the pernigraniline-base (a) and (b), the emeraldine-base (c) and the emeraldine-salt (d). The dash lines represent delocalized entities.

band system with metal-like conduction. The recoiling entities correspond to a mixture of H^+ and “ H^0 ” and proton conduction is allowed. Presumably, free “ H^0 ” and H^+ entities contribute to the observed continuum of intensity and cannot be distinguished. They form a gas with weak electrical-charge density.

In any case, the electronic energy of H^- entities is likely to be much greater than that of “ H^0 ” entities. However, if it were lower than the bottom of the electronic π -band, electrons should be withdrawn from the polymer band to form H^- entities and the emeraldine-base should be an insulator with an empty band. Then, the metal-like conduction of the emeraldine-salt should involve depopulation of the σ -band at lower energy to transform H^+ into “ H^0 ” and/or H^- entities. It is doubtful that metal-like conduction could occur in this case and this scheme is unlikely.

Whereas all protons are free in the emeraldine-base, some of the particles are trapped in shallow potential wells with dissociation threshold $\sim 300 \text{ cm}^{-1}$ above the ground state in the emeraldine-salt. Presumably these are H^+ entities localised by electrostatic interactions nearby the heavy counter-ions (A^-). For highly protonated-salts, as those under investigation, the counter ions are likely to be evenly distributed in order to minimise Coulomb interactions. The shallow potential-well could be a partial view of a quasi-periodic potential extending itself throughout the sample.

At a very low temperature, all protons in the salt are trapped in the shallow wells. Only “ H^0 ” entities should be free and proton conduction is negligible. At room temperature, the dissociation-threshold is such that the continuum is populated and a significant amount of H^+ entities is delocalised (e.g., $\sim 50\%$ at 300 K).

Beside free and thermally delocalised protons, there may be a small amount of bound protons trapped in the structural defects anticipated in such disordered systems. Presumably, they do not contribute significantly to the polymer conductivity. These protons could be involved in hydrogen bonds.

A naive view is that a gas of free hydrogen-atoms such as “ H^0 ” entities should react rapidly to form hydrogen molecules. However, such molecules are not observed despite the great sensitivity of INS,

specifically to this molecule. It transpires that the host polymer prevents the formation of H_2 molecules. Consequently, “ H^0 ” entities are certainly quite different from real free hydrogen atoms.

The INS spectra of hydrated polymers reveal continuums of intensity quite similar to those observed for the dried samples. The spectra look like that of ice and there is no evidence for protonated water-molecules. Apparently, the recoiling entities are specifically associated to the polymer structure and rather insensitive to water molecules. The increase of conduction with the water content could be related to the capability of water molecules to bridge defects in and between the polymer chains.

Different models have been proposed to account for the large variations of electron and proton conductivities in polyanilines. Photoinduced optical studies [47–51] have revealed long-lived massive excitations with $m \sim 60$ electron-mass. These masses and their long time-scale dynamics have been tentatively related to defect-states (polarons and solitons) associated with localised changes of the ring-torsion-angle order-parameter: ring rotation toward planar conformations for polarons and a reversal of the sign of the ring-torsion-angle order-parameter for solitons. Within this general framework, more focused models have been proposed for various oxidation and protonation degrees [45]. It was concluded that both mechanisms should occur simultaneously. The picture for proton and electron conductions in polyanilines which emerges from the INS studies reported above is largely at variance from these views: there is no evidence for single-bond double-bond alternation, as anticipated if protons and electrons were totally delocalised. Further theoretical works including the new dynamics presented above for free protonic entities should give a more realistic view of the electrical properties of polyanilines.

6. Conclusion

INS spectra of the emeraldine-base and salt and their ring-deuterated analogues provide a new insight onto various dynamics. In all samples recoiling entities with mass ~ 1 amu are evidenced. Bands anticipated for the N–H groups, eventually engaged in hydrogen bonds, are not observed with intensities

compatible with the sample stoichiometries. It is concluded that the corresponding protons are largely delocalised. They give the continuum of intensity anticipated for free particles with a mass of 1 amu.

This spectacular result provides insight onto the microscopic mechanism that determines the electronic and protonic conductivities of the emeraldine derivatives. Instead of the conventional representation of polyanilines with mixtures of benzoid and quinoid entities, these polymers are better regarded as the totally conjugated pernigraniline-base structure, with a half-filled electronic conduction-band, interacting with a gas of hydrogen atom-like entities “H⁰”. In the emeraldine-base electrons are transferred from hydrogen atoms to the conduction-band. Consequently, this polymer is a totally-filled band insulator interacting with a gas of free protons H⁺. In the emeraldine-salt electrons are transferred from the totally-filled conduction band to protons to form “H⁰” entities. This polymer has a half-filled band electronic structure with metal-like conduction. Additional protons due to protonation are weakly bound in shallow potential-wells, presumably in the vicinity of the counter-ions (A⁻). At room temperature, these protons are thermally activated and largely free. With the free “H⁰” entities they form a gas of partially charged entities which may account for proton conductivity. All these free entities survive in hydrated polymers.

Polarons and solitons cannot be characterised easily with INS. Even though it is not possible to rule out definitely the existence of such charged defects, the existence of free hydrogen atoms and protons suggests that such defects are very few. Alternative theoretical frameworks are needed to account for the correlations between the protonation degree and the electronic and protonic conductivities of polyanilines.

References

- [1] A.J. Heeger, S. Kivelson, J.R. Schrieffer and W.P. Su, *Rev. Mod. Phys.* 60 (1988) 781.
- [2] R. Kaner and A. MacDiarmid, *Pour Sci.* 126 (1988) 52.
- [3] L.T. Yu, J. Petit, M. Jozefowicz, G. Belorgey and R. Buvet, *C.R. Acad. Sci. Paris* 260 (1965) 5026.
- [4] M. Jozefowicz, G. Belorgey, L.T. Yu and R. Buvet, *C.R. Acad. Sci. Paris* 260 (1965) 6367.
- [5] M.F. Combarel, M. Jozefowicz, G. Belorgey, L.T. Yu and R. Buvet, *C.R. Acad. Sci. Paris* 262 (1966) 459.
- [6] F. Hautière-Cristofini, R. de Surville, M. Jozefowicz, L.T. Yu and R. Buvet, *C.R. Acad. Sci. Paris* 265 (1969) 1346.
- [7] M. Doriomedoff, F. Hautière-Cristofini, R. de Surville, L.T. Yu and R. Buvet, *J. Chim. Phys.* 68 (1971) 1055; I. Mammadou, L.T. Yu and R. Buvet, *C.R. Acad. Sci. Paris, Ser. C* 279 (1994) 931.
- [8] E.M. Genies, A. Boyle, M. Lapkowski and C. Tsintavis, *Synth. Met.* 36 (1990) 139.
- [9] A.G. MacDiarmid, J.C. Chiang, M. Halpern, W.S. Huang, S.L. Mu, N.L.D. Somasiri, W. Wu and S.I. Saniger, *Mol. Cryst. Liq. Cryst.* 121 (1985) 173.
- [10] J.P. Travers, J. Chroboczek, F. Devreux, F. Genoud, M. Nechtschein, A.A. Syed, E.M. Genies and C. Tsintavis, *Mol. Cryst. Liq. Cryst.* 121 (1985) 195.
- [11] A.J. Epstein, J.M. Grinder, F. Zuo, R.W. Bigelon, H.S. Woo, D.B. Tanner, A.F. Richter, W.S. Huang and A.G. MacDiarmid, *Synth. Met.* 18 (1987) 303.
- [12] M. Ohira, T. Sakai, M. Takeushi, Y. Kabayashi and M. Tsuyi, *Synth. Met.* 18 (1987) 347.
- [13] Y. Furukawa, T. Hara, H. Hyodo and I. Harada, *Synth. Met.* 16 (1986) 189.
- [14] F. Wudl, R.O. Angus, Jr., F.L. Lu, P.M. Allemand, D.J. Vachon, M. Nowak and Z.X. Liu, *J. Am. Chem. Soc.* 109 (1987) 3677.
- [15] F. Devreux, G. Bidan, A.A. Syed and Tintavis, *J. Chim. Phys.* 46 (1985) 1595.
- [16] T. Hjertberg, W.R. Salaneck, I. Lundstrom, N.L.D. Somasiri and A.G. MacDiarmid, *J. Polym. Sci. Polym. Lett.* 23 (1985) 503.
- [17] A.F. Richter, A. Ray, K.V. Ramanathan, S.K. Nanohar, G.T. Furst, S.J. Opella, A.G. MacDiarmid and A.J. Epstein, *Synth. Met.*, 29 (1989) E243.
- [18] L.W. Shacklette, J.F. Wolf, S. Gould and R.H. Baughman, *J. Chem. Phys.* 88 (1988) 3955.
- [19] J.M. Ginder, A.F. Richter, A.G. MacDiarmid and A.J. Epstein, *Solid State Commun.* 63 (1987) 97.
- [20] J.C. Chiang and A.G. MacDiarmid, *Synth. Met.* 13 (1986) 193.
- [21] A.J. Epstein, J.M. Ginder, F. Zuo, R.W. Bigelow, H.S. Wood, D.B. Tanner, A.F. Richter, W.S. Huang and A.G. MacDiarmid, *Synth. Met.* 18 (1987) 303.
- [22] W.R. Salaneck, I. Lundstrom, T. Hjertberg, C.B. Duke, E.M. Conwell, A. Paton, A.G. MacDiarmid, N.L.D. Smasiri, W.S. Huang and A.F. Richter, *Synth. Met.* 18 (1987) 285.
- [23] I. Harada, Y. Furukawa and F. Veda, *Synth. Met.* 29 (1989) E303.
- [24] S. Quillard, G. Louarn, J.P. Buisson, S. Lefrant, J. Masters and A.G. MacDiarmid, *Synth. Met.* 49–50 (1992) 525.
- [25] T. Kukuda, H. Takezoe, K. Ishikawa and A. Kukuda, *Synth. Met.* 69 (1995) 247.
- [26] P. Colomban, A. Gruger, A. Novak and A. Régis, *J. Mol. Struct.* 317 (1994) 261.
- [27] A. Gruger, A. Novak, A. Régis and P. Colomban, *J. Mol. Struct.* 328 (1994) 153.
- [28] P. Colomban, A. Gruger and A. Régis, *C.R. Acad. Sci. Paris IIB* 321 (1995) 247.

- [29] J.L. Sauvageol, D. Jurado, A.J. Dianoux, J.E. Fisher, E.M. Scherr and A.G. MacDiarmid, *Phys. Rev. B* 47 (1993) 4959.
- [30] K. Prassides, C.J. Bell, A.J. Dianoux, C.G. Wu and M.G. Kanatzidis, *Physica B*, 180 and 181 (1992) 668.
- [31] C. Fite, Y. Cao and A.J. Heeger, *Solid State Commun.* 70 (1989) 245.
- [32] A. Novak, *Struct. Bonding* 18 (1974) 177.
- [33] A. Lautié, F. Froment and A. Novak, *Spectrosc. Lett.* 9 (1976) 289.
- [34] F. Fillaux and J. Tomkinson, *Chem. Phys.*, 158 (1991) 113.
- [35] F. Fillaux, A. Lautié, J. Tomkinson and G.J. Kearley, *Chem. Phys.* 154 (1991) 135.
- [36] F. Fillaux, H. Ouboumour, J. Tomkinson and L.T. Yu, *Chem. Phys.* 149 (1991) 459.
- [37] F. Fillaux, R. Papoular, A. Lautié and J. Tomkinson, *Fuel* 74 (1995) 865.
- [38] F. Fillaux, R. Papoular, J. Tomkinson and S.M. Bennington, *J. Non-Cryst. Solids* 188 (1995) 161.
- [39] F. Fillaux, S.M. Bennington, J. Tomkinson and L.T. Yu, *Chem. Phys.* 209 (1996) 111.
- [40] J.C. Li, J.D. Londono, D.K. Ross, J.L. Finney, J. Tomkinson and W.F. Sherman, *J. Chem. Phys.* 94 (1991) 6770.
- [41] J.C. Li and D.K. Ross, *J. Phys. Condens. Matter*, 6 (1994) 10823.
- [42] S.W. Lovesey, *International Series of Monographies on Physics* 72. Theory of Neutron Scattering from Condensed Matter Vol. I. Oxford Science Publications (Clarendon Press, Oxford, 1987).
- [43] J. Mayers, C. Andreani and G. Bacioco, *Phys. Rev. B* 39 (1989) 2022.
- [44] J. Tomkinson, *Chem. Phys.* 127 (1988) 445.
- [45] J.M. Ginder and A.J. Epstein, *Phys. Rev. B* 41 (1990) 10674.
- [46] M.G. Roe, J.M. Ginder, P.E. Wigen, A.J. Epstein, M. Angelopoulos and A.G. MacDiarmid, *Phys. Rev. Lett.* 60 (1988) 2789.
- [47] R.P. McCall, J.M. Ginder, J.M. Leng, H.J. Ye, A.J. Epstein, S.K. Manohar, J.G. Masters, G.A. Asturias and A.G. MacDiarmid, *Phys. Rev. B* 41 (1990) 5202.
- [48] M.G. Roe, J.M. Ginder, P.E. Wigen, A.J. Epstein, M. Angelopoulos and A.G. MacDiarmid, *Phys. Rev. Lett.* 14 (1987) 1464.
- [49] R.P. McCall, M.G. Roe, J.M. Ginder, T. Kusomoto, G.E. Asturias, E.M. Scherr, A.G. MacDiarmid and A.J. Epstein, *Synth. Met.* 29 (1989) E433.
- [50] R.P. McCall, J.M. Ginder, M.G. Roe, G.A. Asturias, E.M. Scheer, A.G. MacDiarmid and A.J. Epstein, *Phys. Rev. B* 39 (1989) 10174.
- [51] S.D. Phillips, G. Yu, Y. Cao and A.J. Heeger, *Phys. Rev. B* 39 (1989) 10702.